Water under Pressure

Eric Schwegler, Giulia Galli, and François Gygi
Lawrence Livermore National Laboratory, P.O. Box 808, Livermore, California 94550
(Received 19 May 1999)

Water under pressure is investigated by first principles molecular dynamics, with a focus on the changes in hydrogen bonding and the oxygen network in the nondissociative regime. At a pressure of 10 GPa and a temperature of 600 K, which is close to the freezing point, no appreciable molecular dissociation is observed in the simulations. However, the structure of water is substantially altered from that at ambient conditions. The liquid exhibits a much larger coordination of oxygen atoms, an essential weakening of hydrogen bonding, and sizable changes in the density of electronic states close to the Fermi level. Our results provide new structural data for direct comparison with future experiments.

PACS numbers: 61.50.+p, 61.20.Ja, 61.25.Em, 71.15.Pd

Water has been the subject of numerous experimental and theoretical investigations, given its paramount importance in the physical sciences [1,2] and its key role in life [3]. Nevertheless, many fundamental questions about the properties of water away from ambient conditions are yet unanswered. In particular, most investigations of the effect of compression on the microscopic structure of liquid water have been performed at low (~0.1 GPa) pressures [4], and only a small number of experiments have been performed at pressures up to 2 GPa [5]. For pressures larger than 2 GPa, information on the liquid is even more limited; site-site pair correlation functions and structure factors have not been measured, and structural data are available only from simulations based on empirical potentials [6].

In this Letter, we present first principles molecular dynamics (FP-MD) simulations of water under pressure, before molecular dissociation occurs. At a pressure of 10 GPa and a temperature of 600 K, we find an equilibrium density in excellent agreement with experiment [7], and observe negligible molecular dissociation in accord with shock data [8] and conductivity measurements [9]. In our study, we focus on structural and electronic properties of the liquid and demonstrate how bonding properties are largely modified by pressure, while only moderately affected as temperature is increased by 30%–50% above the melting point.

In the absence of experimentally determined high pressure structural data on water, we choose to employ *ab initio* based methods, which have been proven to be reliable in describing hydrogen bonded systems under various thermodynamic states [10–13]. Semiempirical models, which are usually fitted to reproduce the properties of water at ambient conditions, are biased, and thus may not be appropriate for describing water at high pressure and temperature.

The bulk properties of water are investigated through constant volume and constant pressure simulations of a cubic box containing 54 molecules, subjected to periodic boundary conditions. The nuclear motion is described by Newtonian dynamics, with many body interactions between electrons described by density functional theory [14] in the local density approximation, and with the generalized gradient corrections recently proposed by Perdew *et al.* [15,16]. To make a direct comparison with available experimental data and to determine the accuracy of our theoretical model, we first compute the structural properties of water at ambient conditions ($\rho = 1$ g/cm^3, $T \sim 300$ K) and explore the sensitivity of our results to the choice of the density. The liquid is then heated to a temperature of 600 K and compressed to 10 GPa, which is very close to the experimental freezing point [17].

In Fig. 1, the radial distribution functions (RDFs) at ambient conditions are displayed, along with recent neutron diffraction results [18]. The small dots represent RDFs calculated directly from the atomic trajectories, and the solid lines correspond to the same simulation results after convolution with a Gaussian function, which mimics the experimental broadening that occurs due to the maximum scattering vector ($Q = 16$ Å^{-1}) [18]. This

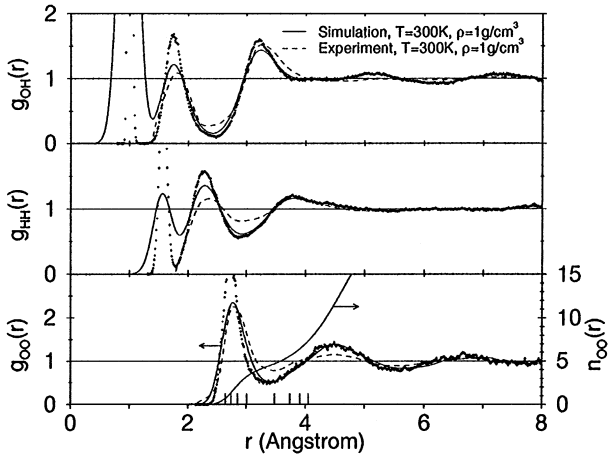

FIG. 1. Radial distribution functions of water at $\rho = 1$ g/cm^3 and 300 K. The dots are simulation data collected directly from the atomic trajectories, the solid lines correspond to the results after convolution with a Gaussian (see text), and the dashed lines are from experiment [24]. The vertical bars indicate the eight smallest average O-O separations. The coordination number $n_{OO}(r)$ is shown for the oxygens.

convolution is essential in making a meaningful comparison to the experimental data that derives from Fourier transformation of measured structure factors [19]. The small differences between the measured and computed RDFs are most likely due to the neglect of proton quantum effects in our simulations. In particular, with an empirical potential and Feynman-Hibbs path integral simulations [20], it has been demonstrated that proton quantum effects decrease the intensity of the first maximum of g_{HH} and increase the first minimum by an amount consistent with the differences observed here. In Fig. 1, the eight smallest oxygen-oxygen interatomic separations averaged over the entire simulation are also shown. Under the first peak in $g_{\mathrm{OO}}(r)$, there is a clustering of four separations that correspond to the nearest neighbor coordination shell around the oxygens. The distribution of oxygen angles ($\angle$OOO) within this coordination shell, which exhibits a peak centered around 109°, clearly indicates a preference for a tetrahedral arrangement in the liquid.

In order to quantify the number of hydrogen bonds present in liquid water, we adopt a purely geometric definition. A hydrogen bond is identified when two oxygen atoms are separated by at most 3.5 Å, and when a hydrogen atom is located between the two oxygens, such that $\angle$OHO is greater than 140°. Although somewhat arbitrary, this definition enables the identification of trends between different simulation conditions. Based on this definition, there are on average 3.5 hydrogen bonds per water molecule in the simulation at ambient conditions, which compares well with a recent analysis of experimental data that indicated 3.58 hydrogen bonds under similar conditions [18].

The static structure factors, $S(k)$, computed directly from the atomic trajectories, are compared to those measured for both deuterated and hydrogenated water in the top two panels of Fig. 2. The agreement between theory and experiment, although not perfect, is very good; the position and intensity of all peaks are reproduced by the theory within a few percent. This straightforward comparison with experiment provides additional evidence that FP-MD can accurately reproduce the characteristic properties of liquid water [10,21]. We also note that although much longer simulation times are needed to precisely measure self-diffusion coefficients [22], a preliminary result of 2.4×10^{-5} cm^2 s^{-1} agrees well with the experimentally observed value of 2.3×10^{-5} cm^2 s^{-1} [23].

At ambient conditions, a precise measurement of pressure (P) is difficult because the relatively small MD cell used in our simulations leads to large fluctuations in the instantaneous value of P. Rather than use a constant P simulation to establish theoretically the equilibrium density, we choose to directly investigate the effect of a small change in the density close to ambient conditions. The volume of the simulation cell is increased by 12% while holding the number of water molecules fixed, and the simulation is repeated as before. Interestingly, we find that peak

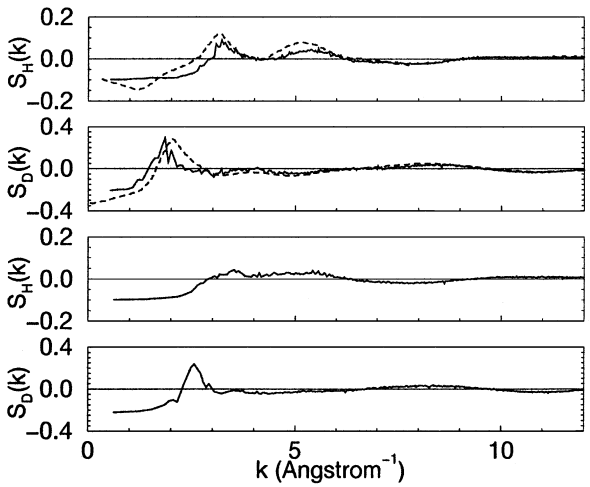

FIG. 2. The static structure factor for light $[S_H(k)]$ and heavy $[S_D(k)]$ water. The top two panels correspond to ambient conditions and the bottom two panels correspond to $\rho = 1.57$ g/cm^3 and $T = 600$. The solid lines are simulation results and the dotted lines are from neutron diffraction.

positions and heights in the RDFs are basically unchanged from those obtained at ambient conditions. Most importantly, we observe a density inhomogeneity in the liquid, and eventually the formation of a small void, which is consistent with the expansion properties of liquid water.

Having established the reliability of our model at ambient conditions, we next carry out a series of simulations at high temperature and pressure. In Fig. 3, the effect of an increase in temperature from 300 to 600 K, at constant density (along an isochore of 0.9 g/cm^3) is shown. Although the intensities of the peaks are reduced, the peak positions remain essentially fixed, with a small outward shift (~0.05 Å) of the first peak in $g_{\mathrm{OO}}(r)$. Furthermore, the $\angle$OOO distribution within the first

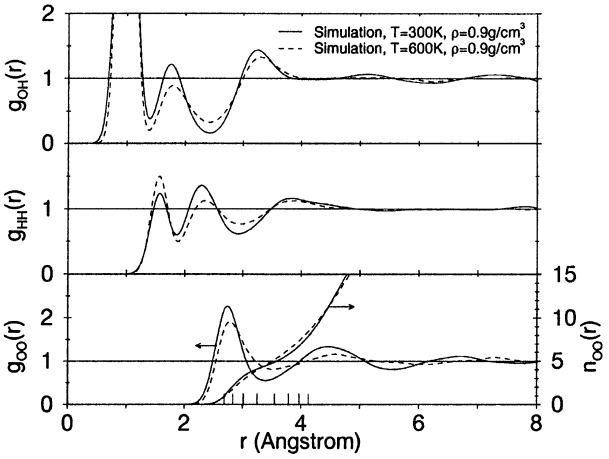

FIG. 3. The effect of temperature on the radial distribution function of water at a density of $\rho = 0.9$ g/cm^3. Solid and dashed lines correspond to convoluted simulation data at 300 and 600 K, respectively. The vertical bars indicate the eight smallest average O-O separations at 600 K. The coordination number $n_{\mathrm{OO}}(r)$ is shown for the oxygens.

coordination shell is very similar at 300 and 600 K, indicating that the tetrahedral arrangement of the liquid persists at 600 K. Despite the rather small changes in the arrangement of oxygen atoms, the average number of hydrogen bonds per water molecule decreases from 3.5 at ambient conditions to 2.9, which reflects the increased thermal motion of the hydrogens.

In Fig. 4, an increase in pressure (from a density of 0.9 to 1.57 g/cm^3) along an isotherm of 600 K is shown to have a much larger effect on the RDFs than an increase in temperature along the chosen isochore. At high pressure, the second peak of $g_{OH}(r)$, occurring at 1.8 Å at low density, is no longer resolved. Even more dramatic, $g_{OO}(r)$ clearly indicates that the nearest neighbor coordination shell around oxygen is significantly altered. This change is caused by a collapse of the second coordination shell. Remarkably, the position of the first maximum in $g_{OO}(r)$ exhibits only a small inward shift (~0.1 Å) as pressure is applied, as compared to a large shift (~0.4 Å) that would occur if all bond distances were to decrease uniformly. The integral of the first peak in $g_{OO}(r)$ up to its first minimum at $r = 3.94$ Å increases from 4.5 at ambient conditions to 12.9 at high pressure. However, the integral of the symmetric part of the peak, i.e., up to $r = 3.2$ Å, yields a coordination number of approximately eight. It is interesting to note that in ice VII, which is a stable form of ice at $P = 10$ GPa and $T < 600$ K, the O-O coordination number is also eight. These findings are consistent with those of water under much lower pressures ($P \leq 0.1$ GPa) [24], indicating that changes in the local structure of the compressed liquid resemble those observed in the solid. The changes in the oxygen network are also qualitatively consistent with those obtained with empirical potentials at a lower density ($\rho = 1.36$ g/cm^3) [6], although classical simulations exhibit O-H correlations quite different from ours. The effect of pressure can also be seen in the $\angle$OOO distribution, which at 10 GPa shows the appearance of a second peak at approximately 60° in addition to the original peak centered at 109° that is observed at low pressures.

The static structure factor, especially that of deuterated water (see Fig. 2), exhibits notable changes as well. The first peak in $S_D(k)$, which originates primarily from O-H intermolecular correlations, is moved to larger k values by 0.8 Å^{-1}, and the shoulder present at low pressure at 4 Å^{-1} is shifted towards smaller values.

Pressure has a small effect on the *number* of hydrogen bonds, as determined by the geometric definition. At 600 K, the number of hydrogen bonds decreases from 2.9 at low P to 2.6 at high P. However, the geometric hydrogen bond definition is not rigorous, and a quantitative statement on the number of hydrogen bonds requires a more sophisticated definition, incorporating charge transfer

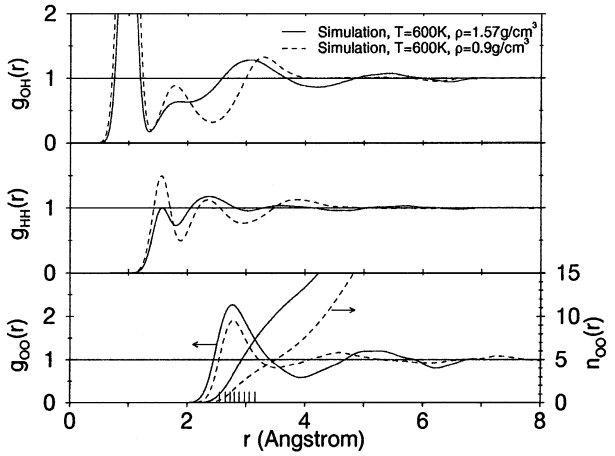

FIG. 4. The effect of pressure on the radial distribution function of water at 600 K. Dashed and solid lines correspond to convoluted simulation data at $\rho = 0.9$ g/cm^3 and $\rho = 1.57$ g/cm^3, respectively. The vertical bars indicate the eight smallest average O-O separations at $\rho = 1.57$ g/cm^3. The coordination number $n_{OO}(r)$ is shown for the oxygens.

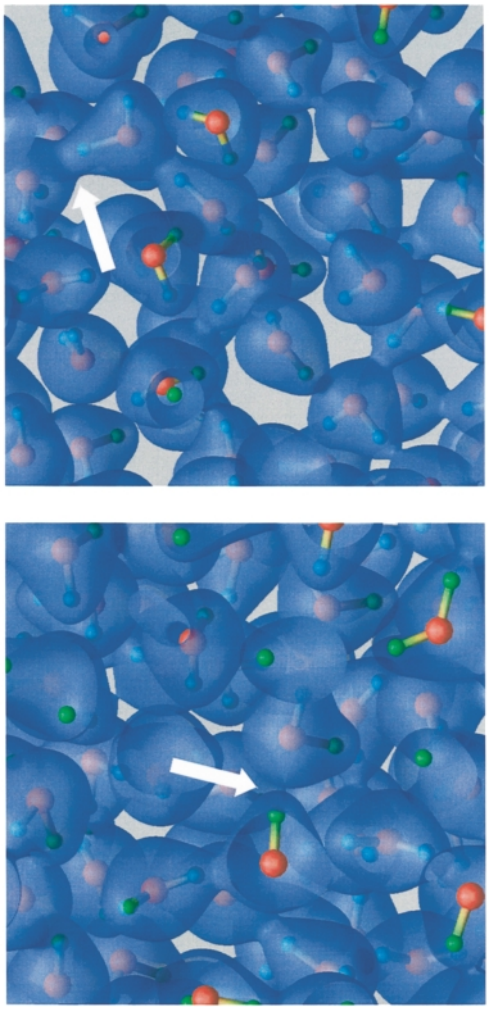

FIG. 5 (color). Isosurfaces (0.035 e/a.u.^{3}) of the charge density. The top panel corresponds to the simulation at $T = 300$ K and $\rho = 0.9$ g/cm^3, and the bottom panel to $T = 600$ K and $\rho = 1.57$ g/cm^3. The arrows indicate regions of interest as discussed in the text.

effects [13]. We qualitatively illustrate this point in Fig. 5, where isosurfaces of the charge density are shown for the low and high P simulations. Close examination of these isosurfaces reveal that at low P pairs of water molecules that satisfy the geometrical hydrogen bond criteria typically also share a region of relatively high charge density. For example, the arrow in the top panel in Fig. 5 points to the region between two water molecules that satisfy the hydrogen bond criteria. However, at high P, pairs of water molecules that are identified as hydrogen bonded by the geometric definition do not necessarily share regions of high charge densities and are often surrounded by disconnected isosurfaces, as indicated by the arrow in the bottom panel in Fig. 5.

Changes in the electronic properties of water upon compression to 10 GPa are also visible in the density of occupied electronic states. In particular, there are substantial modifications in the region near the Fermi level. The valence band width increases by approximately 1 eV and the two highest energy states, associated with oxygen lone-pair electrons, tend to merge with pressure. We note that the essential features observed at 600 K undergo only minor changes when the liquid is heated to 800 K. For example, the diffusion coefficient increases by only a few percent from $\sim 5 \times 10^{-5}$ to 7×10^{-5} cm^2/sec and the essential features of the structure factor shown in the bottom two panels in Fig. 2 are unaltered.

In summary, we have presented the first determination of the structural and electronic properties of water under high pressure, in the nondissociative regime, providing structure factors for direct comparison with future experiments. Our simulations predict that at 10 GPa, the structure of the liquid is remarkably different from that at ambient conditions, with the oxygen coordination almost tripled and substantially weakened hydrogen bonds. The increase in the average oxygen coordination upon melting is much larger at high pressure than at ambient conditions.

We thank W. J. Nellis, N. C. Holmes, F. Ree, M. Colvin, R. Hood, and L. Pizzagalli for useful discussions. This work was performed by the Lawrence Livermore National Laboratory under the auspices of the U.S. Department of Energy, Office of Basic Energy Sciences, Division of Materials Science, Contract No. W-7405-ENG-48.

[1] G. E. Walrafen, in *Water: A Comprehensive Treatise*, edited by F. Franks (Plenum, New York, 1972), Vol. 1.
[2] O. Mishima and H. E. Stanley, Nature (London) **396**, 329 (1998).
[3] M. Gerstein and M. Levitt, Sci. Am. **279**, No. 5, 100 (1998).
[4] O. Mishima and H. E. Stanley, Nature (London) **392**, 164 (1998).
[5] A. Y. Wu, E. Whalley, and G. Dolling, Mol. Phys. **47**, 603 (1982).
[6] F. H. Stillinger and A. Rahman, J. Chem. Phys. **61**, 4973 (1974); R. W. Impey, M. L. Klein, and I. R. McDonald, J. Chem. Phys. **74**, 647 (1981); G. Jancso, P. Bopp, and K. Heinzinger, Chem. Phys. **85**, 377 (1984).
[7] A. C. Mitchell and W. J. Nellis, J. Chem. Phys. **76**, 6273 (1982).
[8] N. C. Holmes, W. J. Nellis, W. B. Graham, and G. E. Walrafen, Phys. Rev. Lett. **55**, 2433 (1985).
[9] S. D. Hamann, in *Modern Aspects of Electrochemistry*, edited by J. O. Bockris and B. E. Conway (Plenum, New York, 1974), Vol. 9.
[10] C. Cavazzoni *et al.*, Science **283**, 44 (1999).
[11] D. R. Hamann, Phys. Rev. B **55**, 10 157 (1997).
[12] M. Benoit, D. Marx, and M. Parrinello, Nature (London) **392**, 258 (1998).
[13] E. D. Isaacs *et al.*, Phys. Rev. Lett. **82**, 600 (1999).
[14] W. Kohn and L. J. Sham, Phys. Rev. A **140**, 1133 (1965).
[15] J. P. Perdew, K. Burke, and M. Ernzerhof, Phys. Rev. Lett. **77**, 3865 (1996).
[16] Electronic wave functions were expanded in a plane wave basis, which was truncated at 80 Ry, and valence-core interactions were described by norm-conserving pseudopotentials. In constant pressure runs, a cutoff of 106 Ry was used to determine the equilibrium density. The code JEEP 1.4.6 (F. Gygi, Lawrence Livermore National Laboratory) was used.
[17] Y. Fei, H. K. Mao, and R. Hemley, J. Chem. Phys. **99**, 5369 (1993).
[18] A. K. Soper, F. Bruni, and M. A. Ricci, J. Chem. Phys. **106**, 247 (1997).
[19] G. Etherington *et al.*, J. Non-Cryst. Solids **48**, 265 (1982).
[20] B. Guillot and Y. Guissani, J. Chem. Phys. **108**, 10 162 (1998).
[21] P. L. Silvestrelli and M. Parrinello, Phys. Rev. Lett. **82**, 3308 (1999).
[22] M. Levitt *et al.*, J. Phys. Chem. B **101**, 5051 (1997).
[23] K. Krynicki, C. D. Green, and D. W. Sawyer, Faraday Discuss. Chem. Soc. **66**, 199 (1978).
[24] M. Canpolat *et al.*, Chem. Phys. Lett. **294**, 9 (1998).